

# Quark Mixing from a Lattice Flavon Model: A Four-Magnitude Parameterization

Vernon Barger<sup>1</sup>

<sup>1</sup>*Department of Physics, University of Wisconsin–Madison, Madison, Wisconsin 53706, USA*  
(Dated: March 3, 2026)

We present the quark weak-mixing component of a Froggatt–Nielsen program, with one flavon and three messengers, in which a single hierarchy parameter  $B$  (with  $\epsilon \equiv 1/B$ ) and a rational-exponent “ $B$ -lattice” organize fermion Yukawa textures. Building on companion mass-fit work, we translate the lattice into sharp predictions for quark mixing. The four-magnitude parameterization serves as a practical interface between the flavon Yukawa textures and quark weak mixing observables, yielding coefficient-free ratio tests of the lattice structure.

## I. INTRODUCTION AND SCOPE

We present the third paper in a flavon/Froggatt–Nielsen [1] trilogy in which a one-flavon plus three-messenger-chain model generates a single hierarchy parameter  $B$  (with  $\epsilon \equiv 1/B$ ) and a rational-exponent “ $B$ -lattice” that organize fermion Yukawa textures. Building on the mass fits established in the first two papers [2, 3], we translate the lattice structure into sharp predictions for weak mixing in the quark sector.

A minimal three-angle plus one-phase Cabibbo–Kobayashi–Maskawa (CKM) [4, 5] parametrization makes the Cabibbo angle an interference between the up- and down-sector  $(1, 2)$  rotations, while CP violation is governed by the same hierarchy through a compact Jarlskog invariant [6]. At a benchmark point motivated by the lattice, the resulting CKM magnitudes and Wolfenstein parameters [7] agree with the Particle Data Group global fit [8] at the quoted precision.

We further exhibit coefficient-cancelling relations in which ratios of CKM elements reduce to pure rational powers of  $B$ , providing multiple independent determinations of the hierarchy parameter from weak-mixing data alone. We restrict attention to the quark sector and CKM mixing, deferring lepton mixing [9, 10] to a separate analysis.

## II. SINGLE- $B$ LATTICE FRAMEWORK

The starting point is a Froggatt–Nielsen (FN) construction [1, 11, 12] in which all fermion mass hierarchies arise from powers of a single small parameter  $\epsilon \equiv 1/B$ . The effective Yukawa matrices may be written schematically as

$$Y_f = C_f \circ \epsilon^{p_f}, \quad (1)$$

where  $p_f$  is a matrix of rational exponents fixed by the  $B$ -lattice and  $C_f$  is a matrix of complex order-one coefficients. The symbol “ $\circ$ ” denotes element-wise multiplication. The frequent restriction to integer FN powers in the literature reflects implicit assumptions of a single abelian symmetry with minimal messenger structure; once these assumptions are relaxed to allow discrete gauge symmetries and lattice charge assignments, rational expo-

nents arise naturally. As shown by Krauss–Wilczek [13], Banks–Dine [14], and Ibáñez–Ross [15], this integer prejudice is not justified. Discrete gauge symmetries can support fractional effective charges, and anomaly cancellation constrains combinations, not individual integers.

The rational-exponent structure encodes the family hierarchy and determines the dominant scaling of masses and mixing angles, while the coefficients  $C_f$  control sub-leading numerical factors and phases. Once the exponent matrices are fixed, the framework becomes highly predictive: entire classes of observables depend only on powers of  $B$ , with limited sensitivity to the detailed coefficient choices.

Diagonalization of the Yukawa matrices proceeds via bi-unitary transformations,

$$Y_f^{\text{diag}} = U_{fL}^\dagger Y_f U_{fR}, \quad (2)$$

and the CKM matrix is given by

$$V_{\text{CKM}} = U_{uL}^\dagger U_{dL}. \quad (3)$$

In this framework, quark mixing arises from the controlled misalignment between the up- and down-sector rotations dictated by the same underlying lattice.

### A. Hierarchy Parameter and Power Counting

It is convenient to adopt a minimal three-angle plus one-phase parametrization of the CKM matrix in which the Cabibbo angle appears as an interference between the  $(1, 2)$  rotations of the up and down sectors.

The Fritzsch–Xing (FX) parameterization [16] of the CKM matrix is

$$V_{\text{CKM}} = R_{12}(\theta_u) R_{23}(\theta) \text{diag}(e^{-i\phi_{\text{FX}}}, 1, 1) R_{12}^\dagger(\theta_d), \quad (4)$$

where  $\theta_u$  and  $\theta_d$  arise from the up- and down-sector  $(1, 2)$  rotations,  $\theta$  is the dominant  $(2, 3)$  mixing angle, and  $\phi_{\text{FX}}$  is the CP-violating phase. This parameterization is exact; the compact relations used here arise from controlled small-angle expansions that are numerically accurate at current experimental precision.

Within the  $B$ -lattice framework, each angle is associated with a definite power of  $\epsilon$ . This implies a hierarchy

$$\theta_d \approx 2.3 \theta_u \approx 4.8 \theta \quad (5)$$

and ensures that CP violation is governed by the same underlying parameter that controls the fermion mass spectrum. The resulting Jarlskog invariant takes a compact form proportional to a simple product of  $B$ -powers, providing a transparent link between flavor hierarchies and CP violation.

In terms of  $s_u \equiv \sin \theta_u$ ,  $s_d \equiv \sin \theta_d$ , and  $s \equiv \sin \theta$  one obtains

$$V_{us} = s_u c_d c - c_u s_d e^{-i\phi_{\text{FX}}}, \quad V_{cb} = s c_u, \quad V_{ub} = s s_u, \quad (6)$$

$$V_{td} = -s s_d, \quad V_{ts} = -s c_d, \quad V_{tb} = c, \quad (7)$$

with  $c \equiv \cos \theta$  and similarly  $c_{u,d} = \cos \theta_{u,d}$ .

The Jarlskog invariant in this parameterization takes the compact form (see Ref. [16])

$$J = s_u c_u s_d c_d s^2 c \sin \phi_{\text{FX}}, \quad (8)$$

making manifest that CP violation is unsuppressed in phase but is suppressed by the hierarchy of the mixing angles.

## B. Input Masses and Scale Choice

Throughout this work we quote running quark masses evaluated at the scale  $M_Z$ . The overall normalization of the Yukawa matrices is fixed by matching the third-family masses,  $m_t(M_Z)$  and  $m_b(M_Z)$ , while the lighter-family masses emerge as predictions controlled by powers of the hierarchy parameter  $\epsilon = 1/B$  and order-one coefficients. Unless stated otherwise, we use

$$m_t(M_Z) \simeq 169 \text{ GeV}, \quad m_b(M_Z) \simeq 2.79 \text{ GeV}, \quad (9)$$

consistent with standard renormalization-group evolution.

With this choice, the up- and down-type mass spectra take the schematic form

$$m_u : m_c : m_t \sim \epsilon^{p_u} : \epsilon^{p_c} : 1, \quad (10)$$

$$m_d : m_s : m_b \sim \epsilon^{p_d} : \epsilon^{p_s} : 1, \quad (11)$$

where the rational exponents  $p_f$  are fixed by the  $B$ -lattice. The numerical agreement of the resulting masses with experiment provides an internal consistency check on the lattice assignment used in the mixing analysis below.

## III. FOUR-MAGNITUDE CKM PARAMETERIZATION

Rather than fitting individual CKM matrix elements independently, we take as input four experimentally well-determined magnitudes,

$$|V_{us}|, \quad |V_{cb}|, \quad |V_{ub}|, \quad |V_{td}|, \quad (12)$$

TABLE I. Mapping between CKM magnitudes and Fritzsche-Xing parameters in the four-magnitude reconstruction.

CKM input	FX parameter
$ V_{ub} / V_{cb} $	$s_u \simeq \sin \theta_u$
$ V_{td} / V_{cb} $	$s_d \simeq \sin \theta_d$
$ V_{cb} $	$s \simeq \sin \theta$
$ V_{us} $	$\phi_{\text{FX}}$ (via Cabibbo interference)

and use them to fix the hierarchy parameter  $B$  and the relative orientation of the up- and down-sector rotations. In the  $B$ -lattice framework, each of these magnitudes is associated with a definite power of  $\epsilon$ , up to order-one coefficients.

A key feature of this approach is that ratios of CKM elements often eliminate the unknown coefficients, yielding relations that depend only on powers of  $B$ . This allows multiple, independent determinations of  $B$  from weak-mixing data alone, providing a stringent test of the single-parameter hypothesis.

For convenience, the direct mapping from four CKM magnitudes to the FX parameters may be written as

$$\boxed{\begin{aligned} s_u &\simeq \left| \frac{V_{ub}}{V_{cb}} \right|, & s_d &\simeq \left| \frac{V_{td}}{V_{cb}} \right|, \\ s &\simeq \frac{|V_{cb}|}{\cos \theta_u} \simeq |V_{cb}|, \\ \cos \phi_{\text{FX}} &= \frac{s_d^2 + s_u^2 - |V_{us}|^2}{2 s_u s_d}, \end{aligned}} \quad (13)$$

Corrections are of relative order  $\mathcal{O}(s^2)$  and are numerically negligible at current precision. The correspondence between CKM inputs and FX parameters is summarized in Table I; supporting analytic identities and empirical regularities used in the reconstruction are collected in Appendix A.

## A. $V_{us}$ from Light-Quark Mass Ratios

The Cabibbo angle arises from an interference between the (1, 2) rotations of the up and down sectors. From the FX parameterization (4), the full interference formula is

$$|V_{us}| \simeq |s_u - s_d e^{-i\phi_{\text{FX}}}|, \quad (14)$$

with the (1, 2) mixing angles governed by light-quark mass ratios,

$$\theta_u \sim \sqrt{\frac{m_u}{m_c}}, \quad \theta_d \sim \sqrt{\frac{m_d}{m_s}}. \quad (15)$$

Within the  $B$ -lattice, both ratios are fixed by powers of  $\epsilon$ , implying that the Cabibbo angle itself is controlled by the same hierarchy parameter that governs the quark mass spectrum.

The phase plays an essential quantitative role. In the real-texture limit ( $\phi_{\text{FX}} = 0$ ), Eq. (14) reduces to the classic Gatto–Sartori–Tonin relation [17, 18]  $|V_{us}| \simeq |\theta_d - \theta_u| \approx 0.114$ , which undershoots the measured value by roughly a factor of two. At the lattice benchmark  $\phi_{\text{FX}} \approx \pi/2$ , the two terms add in quadrature,

$$|V_{us}| \simeq \sqrt{s_d^2 + s_u^2} \approx 0.220, \quad (16)$$

reproducing the observed value [19]. This provides a direct and transparent link between light-quark mass ratios, the CP-violating phase, and the dominant CKM mixing angle.

### B. $V_{cb}$ and the $B$ -Power Relation

In the lattice framework the dominant (2, 3) mixing angle is controlled by a single power of the hierarchy parameter  $\epsilon = 1/B$ . To leading order one finds

$$|V_{cb}| \simeq \theta \sim \epsilon^{p_{cb}}, \quad (17)$$

where the exponent  $p_{cb}$  is fixed by the rational  $B$ -lattice assignment. This relation is largely insensitive to order-one coefficients and therefore provides a particularly clean determination of  $B$  from weak-mixing data.

Using the experimental value of  $|V_{cb}|$ , the inferred value of  $B$  agrees with that obtained from the quark-mass spectrum, providing a nontrivial consistency check of the single-parameter hypothesis.

### C. $V_{ub}$ and $V_{td}$ : Subleading Structure

The remaining small CKM elements,  $V_{ub}$  and  $V_{td}$ , arise from products of the (1, 2) and (2, 3) rotations and therefore probe subleading powers of  $\epsilon$ . Parametrically, one finds

$$|V_{ub}| \sim \theta \theta_u, \quad |V_{td}| \sim \theta \theta_d, \quad (18)$$

up to order-one coefficients.

These relations imply the ratios

$$\frac{|V_{ub}|}{|V_{cb}|} \sim \theta_u, \quad \frac{|V_{td}|}{|V_{cb}|} \sim \theta_d, \quad (19)$$

which depend only on powers of  $B$ . The observed hierarchy between  $|V_{ub}|$  and  $|V_{td}|$  therefore traces directly to the hierarchy between light-quark mass ratios in the up and down sectors.

## D. Summary of CKM Magnitude Relations

Collecting the leading results, the CKM magnitudes satisfy

$$|V_{us}| \sim |s_u - s_d e^{-i\phi_{\text{FX}}}|, \quad (20)$$

$$|V_{cb}| \sim \epsilon^{p_{cb}}, \quad (21)$$

$$|V_{ub}| \sim \epsilon^{p_{cb}} \theta_u, \quad (22)$$

$$|V_{td}| \sim \epsilon^{p_{cb}} \theta_d, \quad (23)$$

with all angles determined by rational powers of the single parameter  $\epsilon = 1/B$ . The success of these relations in reproducing the observed CKM hierarchy provides strong evidence that a single lattice parameter governs both quark masses and mixings.

## IV. CP PHASE AND LATTICE STRUCTURE

### A. Phase Conventions

We adopt a convention in which all CP-violating phases reside in the down-type Yukawa sector. The up-sector Yukawa matrix is taken to be real,

$$\phi_u = \psi_u = 0, \quad (24)$$

so that all physical CP violation originates from the down-sector structure. This choice entails no loss of generality and simplifies the interpretation of the CKM phase.

### B. Two Independent Down-Sector Phases

The down-type Yukawa matrix contains two independent physical phases, denoted  $\phi_d$  and  $\psi_d$ . These phases enter the coefficient matrix  $C^d$  and control the interference pattern responsible for CP violation in the CKM matrix.

The physically meaningful constraint is on the Jarlskog invariant  $J$ , not on the individual phases themselves. Different choices of  $(\phi_d, \psi_d)$  that reproduce the same  $J$  are physically equivalent.

In the convention  $\phi_u = \psi_u = 0$ , the effective phase entering the Cabibbo interference (A1) is determined entirely by the down-sector phases. Diagonalization of the Fritzsch-texture down-type Yukawa matrix produces a left-handed rotation  $U_{d_L}$  whose (1, 2) component acquires a phase from the (1, 2) Yukawa entry (carrying  $\phi_d$ ), while the (2, 3) component acquires a phase from the (2, 3) entry (carrying  $\psi_d$ ). Because  $R_{23}(\theta)$  acts primarily in the (2, 3) sector (with  $\cos \theta \approx 1$  in the (1, 2) block), the Cabibbo element is governed at leading order by the product  $R_{12}(\theta_u) \text{diag}(e^{-i\phi_{\text{FX}}}, 1, 1) R_{12}^\dagger(\theta_d)$ , so the up- and down-sector (1, 2) rotations interfere with a relative phase, producing the interference structure  $e^{i\phi_d} - e^{i\psi_d}$ ;

the difference of two nearby phases is largely imaginary, which naturally drives the FX phase toward  $\pi/2$

$$\phi_{\text{FX}} \equiv \arg(e^{i\phi_d} - e^{i\psi_d}) \quad (25)$$

$$\approx \frac{\pi}{2} \quad (26)$$

The phase  $\phi_{\text{FX}}$  arises from the interference of the two complex rotations and depends only on the relative phase  $\phi_d - \psi_d$ ; the mean phase  $(\phi_d + \psi_d)/2$  is removable by quark-field rephasing.

The retuned factorized shifts used in the down-sector Yukawa benchmark are chosen to restore the down-quark masses at fixed  $(\phi_d, \psi_d)$  while maintaining the FX interference phase at the desired near-maximal value. The CKM verification above is logically orthogonal: the four-magnitude  $B$ -power relations fix the CKM hierarchy and, together with  $\Phi_{\text{FX}}$ , the CP-violating scale, while discrete retunes of the factorized shifts control the detailed quark-mass spectrum without altering the leading CKM power counting.

A benchmark choice of phases (in radians) that reproduces the quark masses and the four CKM magnitudes is

$$\phi_u \simeq 0, \quad \psi_u \simeq 0, \quad \phi_d \simeq 2.8596, \quad \psi_d \simeq 3.540. \quad (27)$$

### C. Rational Shift Vectors

To implement the lattice structure at the coefficient level, we introduce rational shift vectors  $\Delta, \Delta'$  that modify the exponents of selected Yukawa entries. These reproduce the observed quark masses and CKM magnitudes while preserving the underlying lattice relations.

The shift vectors define corresponding matrices  $\Delta_d$  and  $\Delta'_d$  that enter the down-type Yukawa matrix as

$$Y_d = C^d \circ \epsilon^{p_d + \Delta_d + \Delta'_d}. \quad (28)$$

The explicit form of these matrices encodes the effect of the shifts while maintaining rational exponents throughout; the benchmark exponent and shift matrices are given in Appendix B.

### D. FX CP Phase and Its PDG Counterpart

The lattice framework implies a preferred value for the effective CKM phase  $\phi_{\text{FX}}$ , defined through the interference of the down-sector phases. This phase governs CP violation through the Jarlskog invariant rather than through direct identification with a particular CKM angle.

At the benchmark point, the preferred value

$$\phi_{\text{FX}} \approx \frac{\pi}{2} \quad (29)$$

corresponds to maximal CP violation in the sense of maximizing  $J$  for fixed CKM magnitudes.

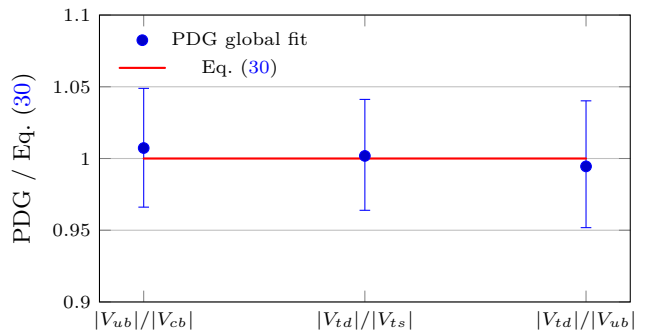


FIG. 1. Comparison of the sharp FX ratio predictions in Eq. (30) with the PDG global-fit magnitudes of the CKM matrix. The plotted points show the PDG central values divided by our Eq. (30) predictions; error bars are obtained by propagating the PDG (one-sigma) uncertainties in Eq. (12.27) of the PDG CKM review [8].

The standard PDG phase  $\delta_{\text{CKM}}$  differs numerically from  $\phi_{\text{FX}}$ . This difference reflects the fact that  $\delta_{\text{CKM}}$  is a convention-dependent parameter, whereas  $\phi_{\text{FX}}$  is tied directly to the lattice structure.

The physically meaningful equality is for the Jarlskog invariant, not for the phases themselves.

## V. BENCHMARK FIT AND QUANTITATIVE RESULTS

Using the four CKM magnitudes as input, we determine the phases  $\phi_d$  and  $\psi_d$  that reproduce the observed CP violation. The resulting CKM matrix agrees with global-fit values within quoted uncertainties.

### A. Sharp Ratio Relations

Even before specifying order-one coefficients, Eqs. (6) and (7) imply several clean relations, including

$$\begin{aligned} \frac{|V_{ub}|}{|V_{cb}|} &\simeq \tan \theta_u & \frac{|V_{td}|}{|V_{ts}|} &\simeq \tan \theta_d \\ &\approx 0.088571, & &\approx 0.208343, \\ \frac{|V_{td}|}{|V_{ub}|} &\simeq \frac{s_d}{s_u} & & \\ &\approx 2.311824. & & \end{aligned} \quad (30)$$

Figure 1 displays these three ratios as (PDG)/(Eq. (30)) with  $1\sigma$  uncertainties.

### B. Direct Inversion of FX Angles

A useful feature of the Fritzsche–Xing (FX) factorization is that the *magnitudes* of the measured CKM elements can be inverted directly to obtain the underlying

TABLE II.  $B$  inferred from CKM magnitudes using the  $B$ -scaling relations and the experimental CKM determinations [8].

Estimator	Value
$B_{us/cb} \equiv  V_{us} / V_{cb} $	5.380201
$B_{cb^3/ub^2} \equiv  V_{cb} ^3/ V_{ub} ^2$	5.371547
$B_{ub^{0.5}/us^3} \equiv  V_{ub} ^{1/2}/ V_{us} ^3$	5.332927
$B_{(td/ub)^2} \equiv ( V_{td} / V_{ub} )^2$	5.393975
$B_{V_{us}} \equiv  V_{us} ^{-9/8}$	5.355434
$B_{V_{cb}} \equiv  V_{cb} ^{-9/17}$	5.368532
$B_{V_{ub}} \equiv  V_{ub} ^{-3/10}$	5.368984
$B_{V_{td}} \equiv  V_{td} ^{-6/17}$	5.364586

effective angles  $(\theta_u, \theta_d, \theta)$  up to small  $\mathcal{O}(s^2)$  corrections:

$$\begin{aligned} \tan \theta_u &\simeq \left| \frac{V_{ub}}{V_{cb}} \right| \simeq B^{-13/9}, \\ \tan \theta_d &\simeq \left| \frac{V_{td}}{V_{ts}} \right| \simeq B^{-17/18}, \\ \sin \theta &\simeq \frac{|V_{cb}|}{\cos \theta_u} \simeq |V_{cb}| \simeq B^{-17/9}. \end{aligned} \quad (31)$$

The  $B$ -scaling values at  $B = 75/14$  are

$$\theta_u \simeq 5.09^\circ, \quad \theta_d \simeq 11.6^\circ, \quad \theta \simeq 2.40^\circ. \quad (32)$$

From Equation (8), the numerical value of the Jarlskog parameter is

$$J \simeq 3.1 \times 10^{-5} \sin \phi_{\text{FX}} \simeq B^{-37/6} \sin \phi_{\text{FX}}. \quad (33)$$

At the benchmark phase  $\phi_{\text{FX}} \simeq 93^\circ$  (for which  $\sin \phi_{\text{FX}} \simeq 1.00$ ), this yields

$$J \simeq 3.1 \times 10^{-5}, \quad (34)$$

in close agreement with the PDG global-fit value  $J = (3.08^{+0.13}_{-0.13}) \times 10^{-5}$  [8].

### C. $B$ -identities from CKM ratios

Several CKM ratios provide direct determinations of  $B$  with weak sensitivity to unknown  $\mathcal{O}(1)$  coefficient magnitudes. A representative set is

$$\begin{aligned} \frac{|V_{us}|}{|V_{cb}|} = B, & \quad \frac{|V_{cb}|^3}{|V_{ub}|^2} = B, \\ \frac{|V_{ub}|^{1/2}}{|V_{us}|^3} = B, & \quad \left( \frac{|V_{td}|}{|V_{ub}|} \right)^2 = B. \end{aligned} \quad (35)$$

The agreement between quark masses, CKM magnitudes, and CP violation provides a nontrivial consistency check of the single- $B$  lattice hypothesis; the numerical values of  $B$  inferred from each estimator are collected

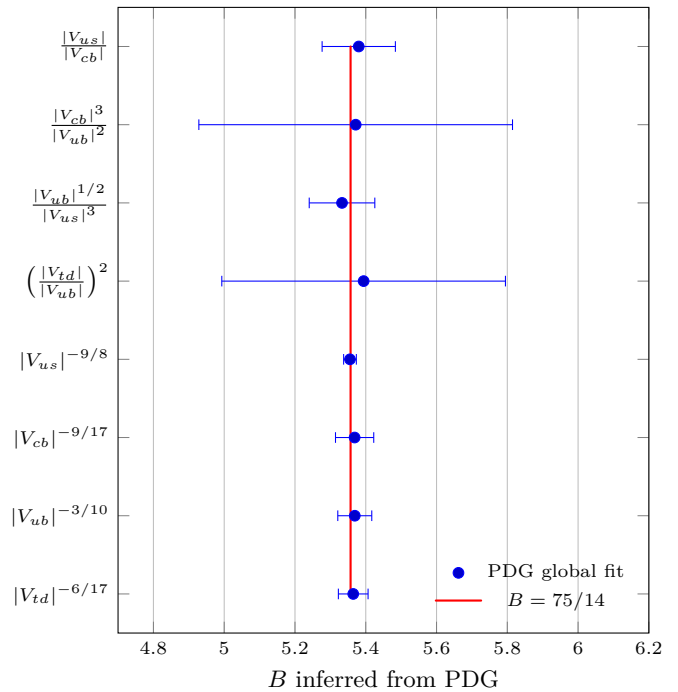


FIG. 2.  $B$  inferred from CKM magnitudes using the PDG Standard-Model global-fit values (unitarity imposed), with  $1\sigma$  error bars from standard propagation. The vertical reference line is drawn at  $B = 75/14 \simeq 5.357$ .

in Table II and displayed graphically in Figure 2. No additional small parameters are required.

It is important to distinguish two classes of predictions within the lattice framework. The coefficient-cancelling ratio relations in Eq. (35) and the sharp FX angle ratios in Eq. (30) are genuinely parameter-free: they follow from the rational exponent lattice alone and are insensitive to the order-one coefficient matrices  $C_f$ . By contrast, the individual CKM magnitudes in Table III and the CP-violating phase depend on the benchmark shift matrices  $(\Delta, \Delta')$  and the fitted phases  $(\phi_d, \psi_d)$ . The strongest evidence for the single- $B$  hypothesis therefore comes from the ratio tests, which provide multiple independent, coefficient-free determinations of  $B$  from weak-mixing data.

## VI. NUMERICAL $B$ -SCALING OF CKM MAGNITUDES

A central phenomenological consequence of the lattice-flavon framework is that quark flavor hierarchies are organized by a single parameter

$$B \equiv \epsilon^{-1}, \quad \epsilon \ll 1, \quad (36)$$

with rational powers fixed by the lattice/messenger structure. For CKM magnitudes we obtain simple  $B$ -power relations of the form

$$|V_{ij}| \sim B^{-p_{ij}} \quad (37)$$

TABLE III. B–power values for CKM magnitudes at  $B = 75/14$ . Experimental values are from the PDG global fit (unitarity imposed) [8]. The powers  $p_{ij}$  in  $|V_{ij}| = B^{-p_{ij}}$  are directly traceable to the  $B^{-n}$  integer scaling of 2-over-2 masses [3].

Element	$B^{-p_{ij}}$	B-scaling	Experiment
$ V_{us} $	$B^{-8/9}$	0.2249	$0.22500 \pm 0.00067$
$ V_{cb} $	$B^{-17/9}$	0.0420	$0.04182^{+0.00085}_{-0.00074}$
$ V_{ub} $	$B^{-10/3}$	0.00372	$0.00369 \pm 0.00011$
$ V_{td} $	$B^{-17/6}$	0.00860	$0.00857^{+0.00020}_{-0.00018}$

where the  $p_{ij}$  values are given in Table III for the benchmark  $B$ -value

$$B = \frac{75}{14} \simeq 5.357. \quad (38)$$

### A. Four Magnitudes as Rational B-Powers

At leading order, the four CKM magnitudes are reproduced by the compact set of rational exponents in the second column of Table III.

These relations capture the observed strong hierarchy  $|V_{us}| \gg |V_{cb}| \gg |V_{ub}|$  while tying it to a single organizing parameter rather than independent small numbers.

### B. Numerical Illustration at $B = 75/14$

The resulting CKM magnitudes are given in the third column of Table III. This demonstrates that a single  $B$  with rational exponents can account for the four measured CKM magnitudes to good accuracy.

The quantitative agreement may be assessed via

$$\chi^2 = \sum_i \frac{(|V_{ij}|_{\text{pred}} - |V_{ij}|_{\text{exp}})^2}{\sigma_i^2} \simeq 0.17 \quad (39)$$

for the four magnitudes in Table III, using the PDG global-fit values [8]. If the lattice exponents are taken as given and  $B$  is the single free parameter, the three remaining degrees of freedom yield  $\chi^2/\text{dof} \simeq 0.06$  ( $p \approx 0.98$ ), with all four elements agreeing to better than  $0.3\sigma$ .

### C. Comparison with the Wolfenstein Expansion

It is instructive to compare this B–scaling organization with the Wolfenstein parameterization (see Table IV), in which CKM hierarchies are expanded in powers of the empirical parameter  $\lambda \simeq |V_{us}| \approx 0.22$ , with additional coefficients ( $A, \rho, \eta$ ) encoding subleading structure and CP violation. The associated unitarity-triangle angles in our flavon-messenger model are

$$(\alpha, \beta, \gamma) \approx (92.04^\circ, 22.55^\circ, 65.40^\circ). \quad (40)$$

TABLE IV. Wolfenstein parameters (and the unitarity-triangle apex) compared with the PDG global fit and the PDG fit using only tree-level inputs.

	This work	PDG global fit [8]
$\lambda$	0.224989	$0.22501 \pm 0.00068$
$A$	0.829702	$0.826^{+0.016}_{-0.015}$
$\bar{\rho}$	0.159760	$0.1591 \pm 0.0094$
$\bar{\eta}$	0.348971	$0.3523^{+0.0073}_{-0.0071}$

TABLE V. Key weak-mixing results and tests in the  $B$ -lattice framework.

Observable	This work	Notes
Hierarchy pattern	$ V_{us}  \gg  V_{cb}  \gg  V_{ub} ,  V_{td} $	fixed by lattice
Improved powers	$ V_{us}  \sim \epsilon^{8/9},  V_{cb}  \sim \epsilon^{17/9}$ $ V_{ub}  \sim \epsilon^{10/3},  V_{td}  \sim \epsilon^{17/6}$	see text
$B$ from ratios	$ V_{us} / V_{cb}  = B,$ $( V_{td} / V_{ub} )^2 = B, \dots$	Eq. (35)
Cabibbo interference	$ V_{us}  \simeq  s_u - s_d e^{-i\phi_{\text{FX}}} $	Eq. (A1)
Phase relation	$\sin \phi_{\text{FX}} \simeq \frac{ V_{cb}  V_{us} \sqrt{1- V_{us} ^2}}{ V_{td} }$	Eq. (A3)
Full CKM	all 9 $ V_{ij} $ within $0.3\sigma$	Table VI
$ V_{ts} $ prediction	0.04128 vs. PDG 0.04110	+0.2 $\sigma$
Jarlskog invariant	$J \simeq 3.1 \times 10^{-5}$	PDG: $(3.08 \pm 0.13) \times 10^{-5}$
$B$ sensitivity	$B = 5.345\text{--}5.373$ ( $1\sigma$ )	Fig. 3

In the present framework, the analogous ordering emerges from a UV–motivated parameter  $B = \epsilon^{-1}$  with rational exponents fixed by lattice/messenger data: for example,  $|V_{us}| \sim B^{-8/9}$ ,  $|V_{cb}| \sim B^{-17/9}$ , and  $|V_{ub}| \sim B^{-10/3}$  reproduce the familiar Wolfenstein pattern while providing a dynamical origin for it. Thus the Wolfenstein expansion may be viewed as an effective description that can arise from an underlying lattice structure governed by a single organizing parameter  $B$ ; the explicit  $B$ -scalings of the Wolfenstein parameters are derived in Appendix C.

### D. Full $3 \times 3$ CKM Reconstruction

Although only four magnitudes are used as input to fix the FX parameters, the reconstruction determines the entire  $3 \times 3$  CKM matrix. Table VI compares all nine predicted magnitudes with the PDG global-fit values [8].

Every element agrees with the PDG determination to better than  $0.3\sigma$ . The total  $\chi^2$  for all nine magnitudes is  $\chi^2 \simeq 0.3$ , corresponding to a  $p$ -value well above 0.99.

Of the five predicted (non-input) elements,  $|V_{ts}|$  provides a particularly useful test. In the FX parameterization  $|V_{ts}| = s c_d$ , which to leading  $B$ -power gives  $|V_{ts}| \sim B^{-17/9}$ , the same scaling as  $|V_{cb}| = s c_u$ . The two differ only through the ratio  $c_d/c_u = \cos \theta_d/\cos \theta_u \simeq 0.983$ ,

TABLE VI. Full  $3 \times 3$  CKM magnitudes from the four-magnitude FX reconstruction at  $B = 75/14$ , compared with the PDG global fit (unitarity imposed) [8]. Elements marked with ( $\star$ ) are the four inputs; the remaining five are predictions.

Element	This work	PDG global fit	Pull
$ V_{ud} $	0.97438	$0.97435 \pm 0.00016$	$+0.2\sigma$
$ V_{us} ^\star$	0.22490	$0.22500 \pm 0.00067$	$-0.1\sigma$
$ V_{ub} ^\star$	0.00372	$0.00369 \pm 0.00011$	$+0.3\sigma$
$ V_{cd} $	0.22477	$0.22486 \pm 0.00067$	$-0.1\sigma$
$ V_{cs} $	0.97351	$0.97349 \pm 0.00016$	$+0.1\sigma$
$ V_{cb} ^\star$	0.04200	$0.04182^{+0.00085}_{-0.00074}$	$+0.2\sigma$
$ V_{td} ^\star$	0.00860	$0.00857^{+0.00020}_{-0.00018}$	$+0.2\sigma$
$ V_{ts} $	0.04128	$0.04110^{+0.00083}_{-0.00072}$	$+0.2\sigma$
$ V_{tb} $	0.99911	$0.99912 \pm 0.00025$	$-0.0\sigma$

yielding

$$|V_{ts}| \simeq 0.04128, \quad (41)$$

compared with the PDG value  $0.04110^{+0.00083}_{-0.00072}$  ( $+0.2\sigma$ ). Because  $|V_{ts}|$  is not used as input, this constitutes a genuine fifth prediction of the framework.

### E. Unitarity Verification

Since the FX parameterization is an exact factorization of a unitary matrix, the reconstructed CKM matrix satisfies row and column unitarity by construction. We verify this explicitly at the benchmark point:

$$\sum_j |V_{ij}|^2 = 1, \quad \sum_i |V_{ij}|^2 = 1, \quad (42)$$

for all  $i, j$ , to numerical precision ( $|1 - \sum| < 10^{-10}$ ). This provides an internal consistency check on the four-magnitude reconstruction: four inputs are sufficient to fix a unitary  $3 \times 3$  matrix (up to unphysical phases), and the reconstruction is self-consistent.

### F. Sensitivity to $B$

The sharpness of the  $B$  determination can be assessed by scanning  $\chi^2$  over the hierarchy parameter while holding the rational exponents fixed. Figure 3 shows the resulting  $\chi^2$  profile for the four CKM magnitudes in Table III. The minimum lies at  $B \simeq 5.359$  with  $\chi^2_{\min} \simeq 0.13$ , and the lattice value  $B = 75/14$  sits within  $\Delta\chi^2 < 0.02$  of the minimum. The  $1\sigma$  range ( $\Delta\chi^2 = 1$ ) is

$$B = 5.345\text{--}5.373 \quad (1\sigma), \quad (43)$$

corresponding to a fractional uncertainty of  $\pm 0.3\%$ . The  $\chi^2$  rises steeply outside this range: by  $B = 5.28$  or

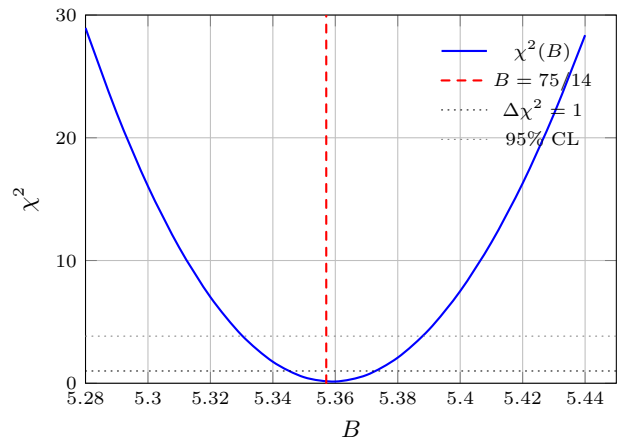


FIG. 3.  $\chi^2$  for the four  $B$ -power CKM magnitude predictions in Table III as a function of  $B$ , using PDG global-fit values [8]. The minimum  $\chi^2 \simeq 0.13$  occurs at  $B \simeq 5.359$ , consistent with  $B = 75/14 \simeq 5.357$  (dashed red line). The  $\Delta\chi^2 = 1$  interval yields  $B = 5.345\text{--}5.373$ ; the 95% CL interval ( $\Delta\chi^2 = 3.84$ ) gives  $B = 5.330\text{--}5.388$ . The steep parabolic profile demonstrates that the four CKM magnitudes tightly constrain  $B$  to within  $\pm 0.3\%$  at  $1\sigma$ .

5.44 the fit is excluded at the  $5\sigma$  level. This tight constraint from CKM data alone, consistent with the value extracted independently from the quark mass spectrum [2, 3], provides strong quantitative evidence for the single- $B$  lattice hypothesis.

## VII. CONCLUSION

We have shown that quark masses, CKM magnitudes, and CP violation can be simultaneously understood within a single- $B$  lattice framework in which rational exponents and controlled phase structure replace arbitrary textures. The  $B$ -scaling description traces both the magnitudes and CP-violating structure of the CKM matrix to a common lattice origin, as summarized quantitatively in Table V. The four-magnitude parameterization provides a compact and practical tool for CKM analysis, enabling direct extraction of the underlying mixing angles and phase from measured observables.

The full  $3 \times 3$  CKM reconstruction (Table VI) yields all nine magnitudes in agreement with the PDG global fit to better than  $0.3\sigma$ , with a total  $\chi^2 \simeq 0.3$  for nine elements. The Jarlskog invariant  $J \simeq 3.1 \times 10^{-5}$  agrees with experiment, and the  $\chi^2$  profile in  $B$  (Figure 3) constrains the hierarchy parameter to  $\pm 0.3\%$  from CKM data alone, consistent with the value obtained independently from quark masses. The success of these predictions motivates further exploration of leptonic mixing and possible ultraviolet completions, which we defer to future work.

## Appendix A: Useful Analytical and Empirical Relations

This Appendix collects some useful analytic identities and empirical regularities in the four-magnitude CKM reconstruction.

### 1. Four-magnitude reconstruction in the Fritzsch–Xing form

The CKM matrix in the minimal three-angle plus one-phase FX form may be parameterized in terms of  $s_u \equiv \sin \theta_u$ ,  $s_d \equiv \sin \theta_d$ ,  $s \equiv \sin \theta$  and the single physical phase  $\phi_{\text{FX}}$ . To leading order in the small angles, the Cabibbo element is governed by interference,

$$|V_{us}| \simeq |s_u - s_d e^{-i\phi_{\text{FX}}}| \quad (\text{to leading order in } s, s_{u,d}), \quad (\text{A1})$$

while the remaining magnitudes reduce to the direct identifications

$$|V_{cb}| \simeq s, \quad |V_{ub}| \simeq s s_u, \quad |V_{td}| \simeq s s_d. \quad (\text{A2})$$

### 2. Approximate relation between $\delta_{\text{PDG}}$ and $\phi_{\text{FX}}$

Equating the Jarlskog invariant  $J$  across phase conventions yields an approximate but accurate relation connecting the PDG phase  $\delta_{\text{PDG}}$  to the FX phase  $\phi_{\text{FX}}$ :

$$\sin \phi_{\text{FX}} \simeq \sin \delta_{\text{PDG}} \frac{|V_{cb}| |V_{us}| \sqrt{1 - |V_{us}|^2}}{|V_{td}|}. \quad (\text{A3})$$

This emphasizes that the physically meaningful equality is for  $J$ , not for the phases themselves.

### 3. Empirical CKM magnitude relations and the unitarity question

The observed quark mixing exhibits additional numerical regularities beyond the basic Wolfenstein hierarchy. Grossman and Ruderman (GR) [20] identified approximate relations among CKM magnitudes,

$$|V_{td}|^2 \simeq |V_{cb}|^3, \quad |V_{ub}|^2 |V_{us}| \simeq |V_{cb}|^4, \quad (\text{A4})$$

which hold at the few-percent level for PDG global-fit magnitudes. We further note the additional empirical correlation

$$|V_{cb}| |V_{ub}|^{1/2} \simeq |V_{us}|^4. \quad (\text{A5})$$

The above empirical relations are useful for constructing multiple ‘‘coefficient-clean’’ estimators of the underlying hierarchy parameter  $B$ .

*a. Relation to B-scaling.* All three relations follow *exactly* from the  $B$ -power assignments in Table III: the first gives  $B^{-17/3} = B^{-17/3}$ , the second  $B^{-68/9} = B^{-68/9}$ , and the third  $B^{-32/9} = B^{-32/9}$ . That the exponents match identically—and not merely to a few percent—means the GR relations are built into the lattice structure rather than being approximate numerical coincidences.

*b. Are these relations consequences of unitarity?* A  $3 \times 3$  unitary CKM matrix contains four physical parameters (three angles and one phase). Once four well-measured magnitudes are specified, unitarity fixes the remaining elements, so one might ask whether the GR relations are automatic. They are not. Expressed in Wolfenstein language, the first relation requires  $r_t^2/A = 1$  and the second requires  $r_u^2/(A^2\lambda) = 1$ , where  $r_{u,t}$  parametrize the unitarity-triangle sides. These are nontrivial constraints on the Wolfenstein parameters ( $A, \bar{\rho}, \bar{\eta}$ ) that are not imposed by unitarity alone; a generic unitary CKM matrix with the measured  $\lambda$  and  $A$  need not satisfy them.

*c. The lattice as a dynamical origin.* Grossman and Ruderman concluded that their relations may point to ‘‘deeper structure’’ but could not exclude an  $\mathcal{O}(10\%)$  accident. The  $B$ -lattice framework resolves this ambiguity: the rational exponents  $p_{ij}$  predict specific values of  $A = \epsilon^{1/9}$ ,  $r_u = \epsilon^{5/9}$ , and  $r_t = \epsilon^{1/18}$  (Appendix C), which automatically enforce  $r_t^2/A = 1$  and  $r_u^2/(A^2\lambda) = 1$ . The GR relations therefore emerge as *derived consequences* of the lattice charge assignments rather than independent empirical observations, and their percent-level accuracy in the data constitutes additional evidence for the single- $B$  organizing principle.

## Appendix B: Flavor-Messenger Model Parameters

### 1. Effective quark Yukawa matrices

We use the parameterization

$$(Y_f)_{ij} = \epsilon^{p_{ij}^f} \left[ 1 + e^{i\phi_f} \epsilon^{\Delta_{ij}^f} + e^{i\psi_f} \epsilon^{\Delta'_{ij}^f} \right] \quad (\text{B1})$$

where  $f = u$  or  $f = d$  and the exponent matrices are

$$p_{ij}^u = \frac{1}{9} \begin{pmatrix} 64 & 39 & 27 \\ 55 & 30 & 18 \\ 37 & 12 & 0 \end{pmatrix}, \quad (\text{B2})$$

$$p_{ij}^d = \frac{1}{9} \begin{pmatrix} 37 & 30 & 27 \\ 28 & 21 & 18 \\ 10 & 3 & 0 \end{pmatrix}.$$

The coefficient matrices are

$$C_{ij}^f = 1 + e^{i\phi_f} \epsilon^{\Delta_{ij}^f} + e^{i\psi_f} \epsilon^{\Delta'_{ij}^f} \quad (\text{B3})$$

with  $\epsilon = 1/B$ . The benchmark matrices imply the explicit  $B$ -scaling.

## 2. Matrix forms of the shifts $\Delta, \Delta'$

The benchmark  $3 \times 3$  shift matrices are

$$\Delta^u = \frac{1}{9} \begin{pmatrix} 0 & 3 & 3 \\ 2 & 5 & 5 \\ 1 & 4 & 4 \end{pmatrix}, \quad \Delta'^u = \frac{1}{9} \begin{pmatrix} 2 & 3 & 2 \\ 1 & 2 & 1 \\ 0 & 1 & 0 \end{pmatrix}, \quad (\text{B4})$$

$$\Delta^d = \frac{1}{9} \begin{pmatrix} 5 & 8 & 9 \\ 0 & 3 & 4 \\ 5 & 8 & 9 \end{pmatrix}, \quad \Delta'^d = \frac{1}{9} \begin{pmatrix} 2 & 3 & 2 \\ 1 & 2 & 1 \\ 0 & 1 & 0 \end{pmatrix}. \quad (\text{B5})$$

The angles  $\phi_d$  and  $\psi_d$  in (B1) are determined from a fit to the data on quark masses and CKM mixings; the angles  $\phi_u$  and  $\psi_u$  are set to zero.

### Appendix C: $B$ -Scalings of Wolfenstein Parameters

At leading Wolfenstein order define

$$\lambda \equiv |V_{us}|, \quad A \equiv \frac{|V_{cb}|}{\lambda^2}, \quad r_u \equiv \frac{|V_{ub}|}{A\lambda^3}, \quad r_t \equiv \frac{|V_{td}|}{A\lambda^3}. \quad (\text{C1})$$

In our 2/2 scheme, with  $\epsilon = 1/B$ ,

$$\lambda = \epsilon^{8/9}, \quad A = \epsilon^{1/9}, \quad A\lambda^3 = \epsilon^{25/9}. \quad (\text{C2})$$

It follows that

$$r_u = \epsilon^{5/9} = 0.3936, \quad r_t = \epsilon^{1/18} = 0.9110. \quad (\text{C3})$$

Solving the unitarity-triangle relations

$$r_u^2 = \rho^2 + \eta^2, \quad r_t^2 = (1 - \rho)^2 + \eta^2 \quad (\text{C4})$$

gives

$$\rho = \frac{1 + r_u^2 - r_t^2}{2} = 0.1625, \quad \eta = \sqrt{r_u^2 - \rho^2} = 0.3585. \quad (\text{C5})$$

### Appendix D: Algebraic Dictionary Between FX and PDG CKM Parameters

We give a compact, algebraic dictionary between the Fritsch–Xing (FX) and PDG conventions for the CKM matrix using rephasing-invariant inputs (four magnitudes and the Jarlskog invariant).

#### 1. Definitions

Define

$$\begin{aligned} s_u &= \sin \theta_u, & c_u &= \cos \theta_u, \\ s_d &= \sin \theta_d, & c_d &= \cos \theta_d, \\ s &= \sin \theta, & c &= \cos \theta. \end{aligned} \quad (\text{D1})$$

and the CP phase is  $\phi_{\text{FX}}$ . In the PDG convention  $s_{ij} = \sin \theta_{ij}$ ,  $c_{ij} = \cos \theta_{ij}$  with CP phase  $\delta \equiv \delta_{\text{PDG}}$ . We then define the FX matrix  $V_{\text{CKM}}^{(\text{FX})}$  as

$$\begin{pmatrix} s_u s_d c + c_u c_d e^{-i\phi_{\text{FX}}} & s_u c_d c - c_u s_d e^{-i\phi_{\text{FX}}} & s_u s \\ c_u s_d c - s_u c_d e^{-i\phi_{\text{FX}}} & c_u c_d c + s_u s_d e^{-i\phi_{\text{FX}}} & c_u s \\ -s_d s & -c_d s & c \end{pmatrix} \quad (\text{D2})$$

and the PDG matrix  $V_{\text{CKM}}^{(\text{PDG})}$  as

$$\begin{pmatrix} c_{12}c_{13} & s_{12}c_{13} & s_{13}e^{-i\delta} \\ -s_{12}c_{23} - c_{12}s_{23}s_{13}e^{i\delta} & c_{12}c_{23} - s_{12}s_{23}s_{13}e^{i\delta} & s_{23}c_{13} \\ s_{12}s_{23} - c_{12}c_{23}s_{13}e^{i\delta} & -c_{12}s_{23} - s_{12}c_{23}s_{13}e^{i\delta} & c_{23}c_{13} \end{pmatrix} \quad (\text{D3})$$

## 2. Invariant quantities

From Eq. (D2),

$$\begin{aligned} |V_{ub}| &= s_u s, & |V_{cb}| &= c_u s, \\ |V_{td}| &= s_d s, & |V_{ts}| &= c_d s. \end{aligned} \quad (\text{D4})$$

and

$$|V_{us}| \simeq |s_u c_d c - c_u s_d e^{-i\phi_{\text{FX}}}|. \quad (\text{D5})$$

The Jarlskog invariant is

$$J = s_u c_u s_d c_d s^2 c \sin \phi_{\text{FX}} = s_{12} s_{23} s_{13} c_{12} c_{23} c_{13}^2 \sin \delta. \quad (\text{D6})$$

## 3. Compact dictionary (PDG $\rightarrow$ FX)

Given PDG magnitudes  $\{|V_{us}|, |V_{ub}|, |V_{cb}|, |V_{td}|\}$  and  $\delta$ :

$$\begin{aligned} s &= \sqrt{|V_{ub}|^2 + |V_{cb}|^2}, & \theta_u &= \arctan\left(\frac{|V_{ub}|}{|V_{cb}|}\right), \\ |V_{ts}| &\simeq \sqrt{|V_{ub}|^2 + |V_{cb}|^2 - |V_{td}|^2}, & \theta_d &= \arctan\left(\frac{|V_{td}|}{|V_{ts}|}\right). \end{aligned} \quad (\text{D7})$$

then  $\cos \phi_{\text{FX}}$  and  $\sin \phi_{\text{FX}}$  are given by:

$$\cos \phi_{\text{FX}} = \frac{s_u^2 c_d^2 c^2 + c_u^2 s_d^2 - |V_{us}|^2}{2 s_u c_u s_d c_d c} \quad (\text{D8})$$

$$\sin \phi_{\text{FX}} = \frac{J}{s_u c_u s_d c_d s^2 c}. \quad (\text{D9})$$

The physically meaningful equality is the equality of  $J$ , not the numerical equality of phase angles across conventions.

- 
- [1] C. D. Froggatt and H. B. Nielsen, “Hierarchy of Quark Masses, Cabibbo Angles and CP Violation,” *Nucl. Phys. B* **147**, 277 (1979).
- [2] V. Barger, “One-Flavon Flavor: A Single Hierarchical Parameter  $B$  Organizes Quarks and Leptons at  $M_Z$ ,” *Phys. Rev. D* **113**, 013002 (2026).
- [3] V. Barger, “Two-over-Two Lattice Flavor from a Single Flavon with Three Messenger Chains,” *Phys. Rev. D* (2026), accepted for publication, arXiv:2602.18393 [hep-ph].
- [4] N. Cabibbo, “Unitary Symmetry and Leptonic Decays,” *Phys. Rev. Lett.* **10**, 531 (1963).
- [5] M. Kobayashi and T. Maskawa, “CP Violation in the Renormalizable Theory of Weak Interaction,” *Prog. Theor. Phys.* **49**, 652 (1973).
- [6] C. Jarlskog, “Commutator of the Quark Mass Matrices in the Standard Electroweak Model and a Measure of Maximal CP Nonconservation,” *Phys. Rev. Lett.* **55**, 1039–1042 (1985), doi:10.1103/PhysRevLett.55.1039.
- [7] L. Wolfenstein, “Parametrization of the Kobayashi–Maskawa Matrix,” *Phys. Rev. Lett.* **51**, 1945 (1983), doi:10.1103/PhysRevLett.51.1945.
- [8] Particle Data Group, “Review of Particle Physics,” *Phys. Rev. D* **110**, 030001 (2024).
- [9] B. Pontecorvo, “Inverse beta processes and nonconservation of lepton charge,” *Sov. Phys. JETP* **7**, 172 (1958) [*Zh. Eksp. Teor. Fiz.* **34**, 247 (1957)].
- [10] Z. Maki, M. Nakagawa, and M. Sakata, “Remarks on the unified model of elementary particles,” *Prog. Theor. Phys.* **28**, 870–880 (1962), doi:10.1143/PTP.28.870.
- [11] M. Leurer, Y. Nir, and N. Seiberg, “Mass matrix models,” *Nucl. Phys. B* **398**, 319 (1993).
- [12] M. Leurer, Y. Nir, and N. Seiberg, “Mass matrix models: The Sequel,” *Nucl. Phys. B* **420**, 468 (1994).
- [13] L. M. Krauss and F. Wilczek, “Discrete gauge symmetry in continuum theories,” *Phys. Rev. Lett.* **62**, 1221–1223 (1989).
- [14] T. Banks and M. Dine, “Note on discrete gauge anomalies,” *Phys. Rev. D* **45**, 1424–1427 (1992), arXiv:hep-th/9109045.
- [15] L. E. Ibáñez and G. G. Ross, “Discrete gauge symmetry anomalies,” *Phys. Lett. B* **260**, 291–295 (1991).
- [16] H. Fritzsch and Z. Xing, “On the parametrization of flavor mixing in the standard model,” *Phys. Rev. D* **57**, 594–597 (1998).
- [17] R. Gatto, G. Sartori, and M. Tonin, “Weak self-masses, Cabibbo angle, and broken  $SU(2) \times SU(2)$ ,” *Phys. Lett. B* **28**, 128 (1968).
- [18] R. J. Oakes, “ $SU(2) \times SU(2)$  breaking and the Cabibbo angle,” *Phys. Lett. B* **29**, 683 (1969).
- [19] E. Blucher, G. D’Ambrosio, and W. J. Marciano, “ $V_{ud}$ ,  $V_{us}$ , the Cabibbo angle, and CKM unitarity,” Particle Data Group review (2024 edition; 2025 update).
- [20] Y. Grossman and J. T. Ruderman, “CKM substructure,” *JHEP* **01**, 143 (2021), arXiv:2007.12695 [hep-ph].